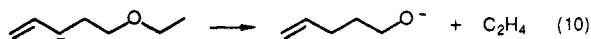$(CH_2)_nOEt$ (n = 1, 2) occur by β-proton transfer to the initial carbanion center followed by alkene elimination to produce the expected alkoxide ion (see eqs 9 and 10). A suggested mechanistic profile for the former reaction is shown in Figure 3; in this case the proton transfer occurs through a six-center state.

$$\text{(9)}$$

$$\text{(10)}$$

Surprisingly, the elimination reaction even occurs when n = 7 (Table I), but as n increases, the competing reactions shown in eqs 11 and 12 increase with respect to the alkene elimination. The formulation of these product ions is rationalized as proceeding through the ion complex d.
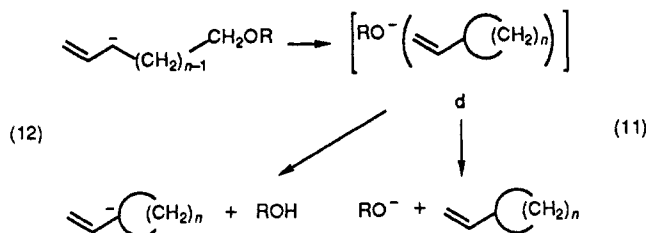
(34) Bartmess, J. E.; Scott, J. A.; McIver, R. T. *J. Am. Chem. Soc.* **1979,** *101,* 6046.

(C) Decompositions of Ions $PhCH(CH_2)_nOR$. A similar but more pronounced effect is noted in the spectra of the phenyl derivatives listed in Table I. Except for $PhCHCH_2OEt$ (where loss of C_2H_4 gives the base peak), elimination of the alkene is less pronounced than formation of RO^-. In this series, the abundance of the peak produced by elimination of the alkene decreases as both n and R increase.

Conclusion

(i) The characteristic decomposition of the species $CH_2=CHCH(CH_2)_nOEt$ (n = 1, 2) is the E1cB elimination of ethene following β-proton transfer to the initial carbanion site. The reaction is most pronounced when the β-proton transfer to the initial carbanion site occurs through a six-center transition state. The elimination process occurs even when n = 7. The latter observation emphasizes the proclivity of proton-transfer reactions in such systems even when the carbanion center is remote from the proton-donor site. (ii) When n = 0, the expected elimination reaction does not occur, i.e., where β-proton transfer to the initial carbanion center requires a five-center state. Instead, proton transfer occurs to the adjacent methine position with the ultimate formation of $(MeCOCH_2)^-$ as the sole ionic species.

L-Edge Spectroscopy of Molybdenum Compounds and Enzymes[f]

G. N. George,[†] W. E. Cleland, Jr.,[‡] J. H. Enemark,[§] B. E. Smith,[‖] C. A. Kipke,[§] S. A. Roberts,[§] and S. P. Cramer*,[⊥]

Contribution from the Corporate Research Science Laboratories, Exxon Research and Engineering Company, Annandale, New Jersey 08801, Department of Chemistry, University of Mississippi, University, Mississippi 38677, Department of Chemistry, University of Arizona, Tucson, Arizona 85721, AFRC Unit of Nitrogen Fixation, University of Sussex, Brighton, UK BN1 9RQ, and National Synchrotron Light Source, Brookhaven National Laboratory, Upton, Long Island, New York 11973. Received January 30, 1989

Abstract: Spectra at the molybdenum L_2 and L_3 edges have been recorded by use of synchrotron radiation and analyzed in terms of ligand field theory. Four distinct p → d transitions were observed in the derivative spectra of molybdenum oxychloride complexes. Comparison with optical data for the same compounds, as well as for Tc analogues, showed that $L_{2,3}$-edge spectra qualitatively reflect the unfilled Mo d-level splittings. A semiempirical correlation scheme, using Racah parameters to correct for exchange and Coulomb interactions, predicted optical splittings with an accuracy of better than 5%. This capability was used to reject certain interpretations of the MoO_4^{2-}, $MoOCl_4(H_2O)^-$, and $MoOCl_5^-$ spectra. Single-crystal spectra for $[N(Et)_4][MoOCl_4(H_2O)]$ helped confirm the assignments. Chemical effects on Mo L-edge spectra were surveyed for LMoOXY compounds, where L represents hydrotris(3,5-dimethyl-1-pyrazolyl)borate and X and Y are various ligands. Spectral sensitivity to oxidation state, terminal oxo vs terminal sulfido ligands, and different halide ions are also compared. Preliminary spectral analysis of several molybdenum enzymes is presented. L_3-edge splittings of 1.72 and 1.40 eV were observed for nitrogenase and active xanthine oxidase, respectively. Oxidized sulfite oxidase gave L_3-edge splittings of 1.05, 2.14, and 3.05 eV. L-edge spectroscopy is a useful technique for studying molybdenum in small molecules, enzymes, and catalysts, especially if such materials are available in oriented forms.

Molybdenum K-edge X-ray absorption has been used for the study of molybdenum enzymes,[1] aqueous solutions,[2] amorphous materials,[3,4] and catalysts.[5] Although the experimental conditions at 20 keV are ideal for EXAFS, utilization of the K-edge XANES

is hindered by the 6-eV natural line width for the K hole.[6] Furthermore, angular momentum selection rules restrict the types of transitions that can be observed at the K edge to final states

(1) Cramer, S. P. *Advances in Inorganic and Bioinorganic Mechanisms;* Sykes, A. G., Ed.; Academic Press: London, 1983; pp 259–316.
(2) Cramer, S. P.; Eidem, P. K.; Paffett, M. T.; Winkler, J. R.; Dori, Z.; Gray, H. B. *J. Am. Chem. Soc.* **1983,** *105,* 799–802.
(3) Cramer, S. P.; Liang, K. S.; Jacobson, A. J.; Chang, C. H.; Chianelli, R. R. *Inorg. Chem.* **1984,** *23,* 1215–1221.
(4) Scott, R. A.; Jacobson, A. J.; Chianelli, R. R.; Pan, W.-H.; Stiefel, E. I.; Hodgson, K. O.; Cramer, S. P. *Inorg. Chem.* **1986,** *25,* 1461–1466.
(5) Clausen, B. J.; Topsoe, H.; Candia, R.; Villadsen, J.; Lengeler, B.; Als-Nielsen, J.; Christensen, F. *J. Phys. Chem.* **1981,** *85,* 3868–3872.
(6) Krause, M. O.; Oliver, J. H. *J. Phys. Chem. Ref. Data* **1979,** *8,* 329–338.

2542 *J. Am. Chem. Soc., Vol. 112, No. 7, 1990*

George et al.

with p character. In contrast, $L_{2,3}$-edge transitions originate at p levels to yield final states of predominantly d or s character. The $L_{2,3}$-edge line widths are 3-fold sharper than the K edges, thereby permitting resolution of d-orbital splittings. In favorable cases, transitions to all unfilled or half-filled d orbitals can be observed, unobscured by charge-transfer bands. Additionally, information about the orientation of particular orbitals in a single crystal or otherwise oriented sample can be obtained from polarization-dependent spectra. Thus, L-edge spectroscopy can provide information about site geometry that complements the radial distance data obtained from K-edge EXAFS.

Despite the advantages of Mo L-edge spectroscopy, until recently this region of the spectrum has not been vigorously exploited.[7] This paper begins with a systematic survey of the experimental aspects of Mo L-edge spectroscopy, including available photon fluxes, natural line widths, and the chemical shift range. The correlation between ligand field effects observed in optical and X-ray spectra is examined for a series of Mo compounds, and an algorithm based on Racah parameters is proposed. The proposed assignments are further tested by using the spectral orientation dependence observed for a $[N(Et)_4][MoOCl_4(H_2O)]$ crystal. Additional small-molecule spectra are then presented to illustrate chemical effects such as oxo vs sulfido groups and halide ion substitution on the spectra. Finally, preliminary Mo L-edge spectra are reported for the Mo enzymes nitrogenase, xanthine oxidase, and sulfite oxidase.

Experimental Section

Data Collection. The data were recorded as fluorescence excitation spectra[8] with a Stern-Heald-Lytle detector[9] at the Stanford Synchrotron Radiation Laboratory on Beam Line VI-2[10] under dedicated conditions (3 GeV, ca. 50 mA), using either Si(111) or Ge(111) monochromator crystals. The 54-pole wiggler magnet was adjusted to undulator mode with a field of from 1.51 to 1.15 kG,[11] or to wiggler mode, with a field of 5 kG.

The measured incident fluxes of 1.0×10^{10} photons/(s eV 50 mA) in undulator mode, and 4.6×10^{10} photons/(s eV 50 mA) under wiggler conditions, compare favorably with values reported for vacuum beam lines.[12,13] Given the significant attenuation by beam-line components, calculated as at most 3.5% transmission at 2500 eV without carbon filters, there is still room for dramatic improvement in the low-energy operation of this beam line.[14]

Data Manipulation and Analysis. The spectra were calibrated vs the first absorption edge peak for sodium thiosulfate, reported as 2469.2 eV by Sekiyama et al.[15] Although the absolute accuracy of this value is not known, edge positions were reproducible to better than 0.1 eV. For the concentrated samples, the edge contribution was isolated from the F/I_0 spectrum by subtraction of a polynomial fit over the preedge region. The data were normalized to unit absorbance change in the region 50 eV beyond the edge.

Because of the large background structure from sulfur EXAFS, the protein spectra required a more complicated background removal. In these cases, two cubic polynomials were fit to the spectrum over 25-eV intervals ending or beginning 12 eV from the center of the edge region. These polynomials were then extrapolated through the edge region and constrained to join smoothly. This cubic spline was then subtracted from the overall spectrum to give an approximate Mo contribution.

Derivatives of L-edge spectra were calculated by fitting cubic polynomials to 0.4-eV regions centered at each data point and calculating the polynomial derivative. Quantitative estimates of line positions were made
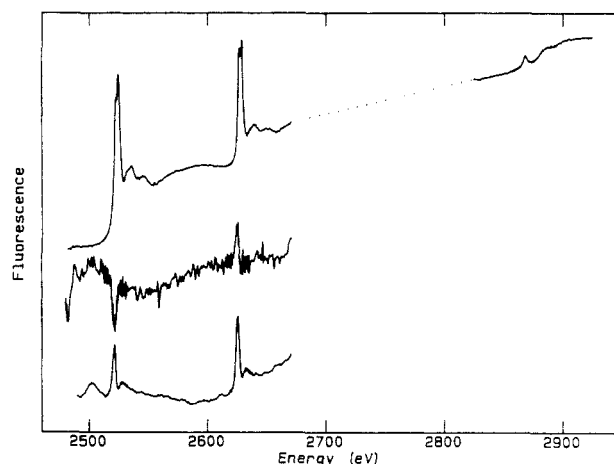

Figure 1. General appearance of L-edge fluorescence excitation spectra. Top to bottom: Na_2MoO_4, $(NH_4)_2MoS_4$, and $(NH_4)_2MoS_4$ diluted with BN.

by curve-fitting the second- or third-derivative spectrum to a sum of Lorentzian line shapes, varying position, amplitude, and width of each component.

Sample Preparation. The model compound spectra were recorded on powdered neat samples lightly dusted onto the adhesive side of a piece of Mylar tape. Air-sensitive compounds were prepared in a nitrogen-filled glovebox and covered with a polypropylene window before transfer to the helium-filled sample chamber.

Oxo- and sulfidomolybdenum(IV) complexes with hydrotris(3,5-dimethyl-1-pyrazolyl)borate, $HB(Me_2pz)_3^-$ or "L", and diethyldithiocarbamate, $(S_2CNEt_2)^-$, ligands were prepared by the literature method.[16] Oxomolybdenum(V) complexes of the form $LMoO(X, Y)$, where $(X, Y) = (Cl^-, Cl^-)$, $(Cl^-, {}^-OMe)$, $(^-OCH(CH_3)CH(CH_3)O^-)$, $(^-SCH_2CH_2O^-)$, $(^-SCH_2CH_2S^-)$, $(^-SC_6H_5)_2$, $(^-OC_6H_5)_2$, $(^-OC_6H_4-o-S^-)$, $(^-OC_6H_4-o-O^-)$, and $(^-SC_6H_3(CH_3)-o-S^-)$ were also prepared by published procedures.[17] $LMoSCl_2$ was prepared by reaction of $LMoOCl_2$ with excess B_2S_3.[18] $MoO_2X(S_2CNEt_2)_2$ (X = Cl^-, Br^-) was prepared as described by Young et al.[19] Dioxomolybdenum(VI) complexes of the form $LMoO_2X$, where X = anions Cl^- or Br^-, were prepared according to Young et al.[20] Dioxomolybdenum(VI) and disulfidomolybdenum(VI) complexes with the anion of N-hydroxypiperidine, or "pip", were prepared by the method of Wieghardt et al.[21]

$Cu_{1.9}Mo_3S_4$ was kindly provided by David Johnson and MoO_3 by Al Rupert, and $(NH_4)_2MoS_4$ was likewise supplied by Drs. Edward Stiefel and Thomas Halbert, all of Exxon Research. $[N(Et)_4][MoOCl_4]$ was prepared by the method of Boorman.[22] Recrystallization from 12 N HCl yielded large single crystals of $[N(Et)_4][MoOCl_4(H_2O)]$. The complex is isomorphous with the corresponding bromide complex,[23] and the crystal used in the study was oriented by X-ray diffraction. The $[PyH]_2$-$[MoOCl_5]$ sample was prepared by the method of Hanson et al.[24]

The protein spectra were recorded at 4 °C on lyophilized samples. Xanthine oxidase, at a concentration of 1 mM in Mo in 50 mM pH 8.2 Bicine buffer before lyophilization, was prepared at the University of Sussex from fresh buttermilk by the salicylate denaturation method.[25] The activity of the preparation corresponded to 75% active Mo centers, calculated according to Bray,[25] which decreased by a further 5% after

(7) Hedman, B.; Frank, P.; Gheller, S. F.; Roe, A. L.; Newton, W. E.; Hodgson, K. O. *J. Am. Chem. Soc.* **1988**, *110*, 3798–3805.

(8) Jaklevic, J.; Kirby, J. A.; Klein, M. P.; Robertson, A. S.; Brown, G. S.; Eisenberger, P. *Solid State Commun.* **1977**, *23*, 679.

(9) Stern, E.; Heald, S. *Rev. Sci. Instrum.* **1979**, *50*, 1579.

(10) Hoyer, E.; et al. *Nucl. Instrum. Methods* **1983**, *208*, 117–125.

(11) Winick, H.; Boyce, R.; Hower, N.; Hussain, Z.; Pate, T.; Umbach, E. *Nucl. Instrum. Methods* **1983**, *208*, 127–137.

(12) Hussain, Z.; Umbach, E.; Shirley, D. A.; Stöhr, J.; Feldhaus, J. *Nucl. Instrum. Methods* **1982**, *195*, 115–131.

(13) Cowan, P. L.; Brennan, S.; Deslattes, R. D.; Henins, A.; Jach, T.; Kessler, E. G. *Nucl. Instrum. Methods* **1986**, *A246*, 154–158.

(14) Tests using an infrared camera to observe the beryllium windows have shown that the thermal load to be considerably less than anticipated. This may permit operation with only 6–10 mils of Be in the beam line: Arthur, J. *SSRL Users' Newsletter* **1987**, (Dec), 6.

(15) Sekiyama, H.; Kosugi, N.; Kuroda, H.; Ohta, T. *Bull. Chem. Soc. Jpn.* **1986**, *59*, 575–579.

(16) Young, C. G.; Roberts, S. A.; Ortega, R. B.; Enemark, J. H. *J. Am. Chem. Soc.* **1987**, *109*, 2938–2946.

(17) Cleland, W. E., Jr.; Barnhart, K. M.; Yamanouchi, K.; Collison, D.; Mabbs, F. E.; Ortega, R. B.; Enemark, J. H. *Inorg. Chem.* **1987**, *26*, 1017.

(18) Young, C. G.; Enemark, J. H.; Collison, D.; Mabbs, F. E. *Inorg. Chem.* **1987**, *26*, 2927–2929.

(19) Young, C. G.; Broomhead, J. A.; Boreham, C. J. *J. Chem. Soc., Dalton Trans.* **1983**, 2135.

(20) Roberts, S. A.; Young, C. G.; Kipke, C. A.; Cleland, W. E., Jr.; Yamanouchi, K.; Enemark, J. H. *Inorg. Chem.*, in press.

(21) Wieghardt, K.; Hahn, M.; Weiss, J.; Swiridoff, W. *Z. Anorg. Allg. Chem.* **1982**, *492*, 164–174.

(22) Boorman, P. M.; Garner, C. D.; Mabbs, F. E. *J. Chem. Soc., Dalton Trans.* **1979**, 1299.

(23) Bino, A.; Cotton, F. A. *Inorg. Chem.* **1979**, *18*, 2710–2713.

(24) Hanson, G. R.; Brunette, A. A.; McDonell, A. C.; Murray, K. S.; Wedd, A. G. *J. Am. Chem. Soc.* **1981**, *103*, 1953–1959.

(25) (a) Hart, L. I.; McGartoll, M. A.; Chapman, H. R.; Bray, R. C. *Biochem. J.* **1970**, *116*, 851–864. (b) Bray, R. C. *Flavins and Flavoproteins*; Massey, V., Williams, C. H., Eds.; Elsevier/North-Holland, Amsterdam, 1982; pp 775–785. (c) Bray, R. C. *The Enzymes*, (3rd Ed.) **1975**, *12*, 299–419.
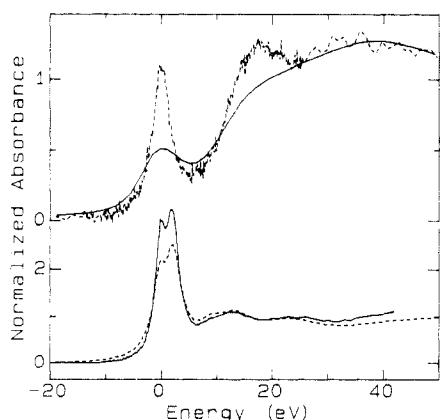
L-Edge Spectroscopy of Mo Compounds and Enzymes

J. Am. Chem. Soc., Vol. 112, No. 7, 1990 2543

Figure 2. Comparison of K and L edges for Na_2MoO_4. Upper curves: K edge (—) vs L_1 edge (---). Lower curves: L_2 edge (—) vs L_3 edge (---). A linear preedge was subtracted in each case, and the data were normalized to unit edge jump beyond the resonance features. The energy scale is with respect to the lowest energy transition.

completion of the X-ray absorption experiments.

The nitrogenase Mo–Fe protein from *Klebsiella pneumoniae* was prepared by established methods,[26] concentrated to 25 mg/mL, and then dialyzed against 25 mM Tris-HCl buffer, pH 7.4, containing 50 mM NaCl and 1 mM $Na_2S_2O_4$. Samples of this preparation were lyophilized anaeorobically. An activity of 1700 nmol of C_2H_2 reduced min^{-1} (mg of protein)$^{-1}$ was measured[26] before lyophilization. Shipping difficulties prevented activity measurements after the measurements, but the spectra were reproduced with different samples on several occasions.

Sulfite oxidase from chicken liver was purified according to Kipke et al.[27] The enzyme activity was verified by the method of Cohen and Fridovich.[28] The concentration of sulfite oxidase heme centers was determined spectrophotometrically by using $\epsilon_{413nm} = 99.9$ mM^{-1} cm^{-1} for the oxidized form of the enzyme.[29] The final fractions pooled from the G-200 column had A_{413}:A_{280} ratios of 0.60 and above. Molybdenum analysis by atomic absorption gave Mo to heme ratios of 1.03:1.00. The enzyme was concentrated to 140 μM in a 20 mM universal buffer consisting of equal concentrations of Tris, Bis-Tris, and Bis-Tris propane, previously adjusted to pH 9 with acetic acid, and lyophilized. Specific activities of better than 35 enzyme units/mg of protein were generally measured before lyophilization, with recovery of better than 90% of activity after redissolving.

Results and Analysis

The general appearance of the fluorescence excitation spectra is illustrated in Figure 1. For concentrated samples such as sodium molybdate, the L_2- and L_3-edge jumps are a significant fraction of the total signal. However, because of its lower oscillator strength and smaller fluorescence yield, the L_1 edge is difficult to observe even under ideal conditions. The influence of fluorescence yield is especially important for samples with large fractions of sulfur, as illustrated with the spectrum of neat $(NH_4)_2MoS_4$, where a negative Mo L_3 edge is observed. This occurs because the 14% sulfur K fluorescence yield is much higher than the 7% Mo $L_{2,3}$ fluorescence yield. As the fraction of photons absorbed by Mo increases, the total fluorescence from the sample decreases, since the Mo reradiates with lower efficiency than S. Diluting the sample with boron nitride, so that the bulk of the absorption is by a nonfluorescent matrix, results in the more conventional positive edge.

Line Widths. The K and L edges for MoO_4^{2-} are compared in Figure 2. The K and L_1 spectra both exhibit a single sharp isolated bound-state transition, which in the former case Kutzler et al. have attributed to a 1s → T_2 transition.[30] Fitting the profile
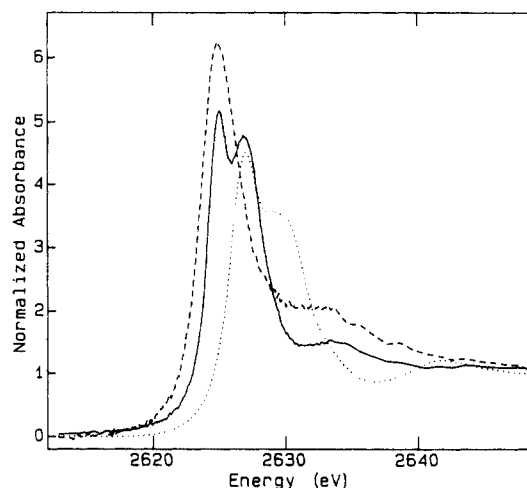

Figure 3. Chemical shift effects for Mo L_2 edges, illustrated with $Cu_{1.9}Mo_3S_4$ (---), $LMoO(S_2CNEt_2)$ (—), and MoO_3 (⋯). The magnitude of the MoO_3 peak may have been reduced by thickness effects.

of this feature, assuming a Lorentzian line shape, gave fwhm line widths of 7.6 eV for the K edge and 3.8 eV for the L_1 edge, after correction for broadening from the monochromator resolution of 4.5 and 0.5 eV, respectively. The lower energy components of the L_3 and L_2 edges were found to have full line widths of 2.1 and 2.3 eV, respectively, assuming 0.4-eV monochromator line widths. The upper bands were 0.45 eV broader, perhaps due to spin–orbit coupling. These values for the Mo L-edge line widths are similar to previously reported values for the fluorescence line widths.[6] As shown in Figure 2, the small line widths of the L_2 and L_3 edges allow resolution of the 2p → E and 2p → T_2 transitions in Na_2MoO_4.

Chemical Shift Range. The Mo K-edge inflection point energy has been shown to correlate with the Mo oxidation state and the covalency of the Mo environment.[31] As illustrated in Figure 3, $L_{2,3}$ edges also exhibit substantial shifts. Among the compounds examined, the lowest L_2 first inflection point fell at 2623.8 eV for $Cu_{1.9}Mo_3S_4$, compared to the highest inflection point of 2626.2 eV for Na_2MoO_4. The observed range of 2.4 eV is substantially smaller than the 10.3-eV range observed for the Mo K edge. However, the smaller natural line width and 10-fold better monochromator resolution makes the L-edge chemical shift more readily measured.

The $Cu_{1.9}Mo_3S_4$ spectrum is also interesting because only a single band is observed. This presumably is a 2p → T_2 transition, with the absence of a 2p → E transition being explained by the filled E subshell for tetrahedral d^4 Mo(II).

Splittings and Correlations with Optical Data. Since optical and $L_{2,3}$-edge spectra both involve d orbitals, there should be some relationship between the splittings observed in both techniques.[32,33] In the "effective Z approximation", the presence of a core–hole will cause the Mo X-ray data to more closely resemble Tc (Z + 1) optical splittings.[34] To further investigate this matter, the spectra for a variety of Mo complexes with known Tc analogues were recorded and analyzed. Although it was possible to model the entire absorption edge region as the sum of Lorentzians (for the bound-state transitions) plus an arctangent (for the continuum contribution), we found it simpler to fit the second- or third-derivative spectra with derivatives of Lorentzians alone. In this case the low curvature arctangent function can be excluded from the fit. Fits with Gaussian line shapes were significantly worse. This procedure is illustrated in Figure 4.

(26) (a) Eady, R. R.; Smith, B. E.; Cook, K. A.; Postgate, J. R. *Biochem. J.* **1972**, *128*, 655–675. (b) Smith, B. E.; Thorneley, R. N. F.; Yates, M. G.; Eady, R. R.; Postgate, J. R. *Proc. Int. Symp. Nitrogen Fixation, 1st* **1976**, 150–176.

(27) Kipke, C.; Enemark, J. H.; Sunde, R. A. *Arch. Biochem. Biphys.* **1989**, *270*, 383–390.

(28) Cohen, H. J.; Fridovich, I. *J. Biol. Chem.* **1971**, *246*, 359–366.

(29) Cohen, H. J.; Fridovich, I. *J. Biol. Chem.* **1971**, *246*, 367–373.

(30) Kutzler, F. W.; Natoli, C. R.; Misemer, D. K.; Doniach, S.; Hodgson, K. O. *J. Chem. Phys.* **1980**, *73*, 3274–3288.

(31) Cramer, S. P. Ph.D. Thesis, Stanford University, 1978.

(32) (a) Sham, T. K.; Brunschwig, B. S. In *EXAFS and Near Edge Structure*; Bianconi, A., Incoccia, L., Stipcich, S., Eds.; Springer-Verlag: Berlin, 1983; pp 168–170. (b) Sham, T. K. *J. Am. Chem. Soc.* **1983**, *105*, 2269–2273.

(33) Hedman, B.; Penner-Hahn, J. E.; Hodgson, K. O. *EXAFS and Near Edge Structure III*; Hodgson, K. O., Hedman, B., Penner-Hahn, J. E., Eds.; Springer-Verlag: Berlin, 1984; pp 64–66.

(34) Parratt, L. G. *Phys. Rev.* **1939**, *56*, 444–448.

Table I. Molybdenum L-Edge X-ray vs Optical Splittings

Mo complex	Tc analogue	Mo, Tc ground state	opt transition or splitting	opt energy, eV		X-ray splitting,[k] eV		pred Mo opt energy, eV
				Mo	Tc	L_3	L_2	
$MoO_4{}^{2-}$	$TcO_4{}^-$	d^0, d^0	$E - T_2$	1.68,[a] >2.5[b]	2.35[c]	2.48	2.19	2.34
	$TcO_4{}^{2-}$	d^1	$E - T_2$		2.10[g]			
$MoS_4{}^{2-}$	*l*	d^0	$E - T_2$	1.25[c]		1.41	1.32	1.36
Mo $OCl_4(H_2O)^-$	$TcOCl_4{}^-$	d^1, d^2	$d_{xy} \rightarrow d_{xz,yz}$	1.66[d]	1.59[h]	1.21	0.58	1.84
			$d_{xy} \rightarrow d_{z^2-y^2}$	2.82[d]		2.83	2.37	3.14
			$d_{xy} \rightarrow d_{z^2}$			4.28	3.71	5.07
$MoOCl_5{}^{2-}$	$TcOCl_5{}^{2-}$	d^1, d^2	$d_{xy} \rightarrow d_{xz,yz}$	1.71[e]	1.32[i]	1.21	0.78	1.94
			$d_{xy} \rightarrow d_{z^2-y^2}$	2.78[e]	2.07,[i] 2.55[i]	2.85	1.99	2.96
			$d_{xy} \rightarrow d_{z^2}$			4.49	3.86	5.25
$LMoOCl_2$	$LTcOCl_2$	d^1, d^2	$\phi_1 \rightarrow \phi_{2,3}$	1.76[f]	1.58[j]	1.26	0.90	2.03
			$\phi_1 \rightarrow \phi_4$			3.24	2.86	3.59
						4.76	4.40	5.66
$LMoSCl_2$	*l*	d^1	$\phi_1 \rightarrow \phi_{2,3}$	1.13[g]		(2.64)[m]	(2.57)[m]	

[a] Reference 35. [b] Reference 36. [c] Reference 49. [d] Reference 50. [e] Reference 51. [f] Reference 18. [g] Reference 52. [h] Reference 53. [i] Reference 54. [j] Reference 55. [k] Estimated accuracy ±0.05 eV. [l] Analogue not known. [m] Average splitting.
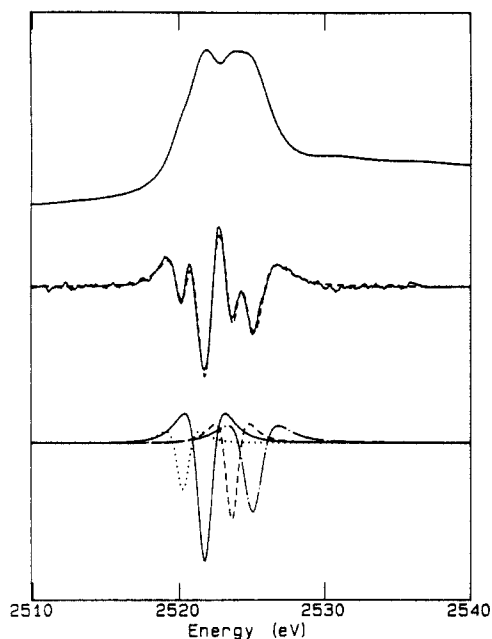

Figure 4. Analysis procedure used for quantitation of $L_{2,3}$-edge spectra, illustrated for $LMoO(^-SCH_2CH_2O^-)$. Top to bottom: normalized absorbance curve; second-derivative curve (—) and best fit (---); individual derivative components.

Figure 5. L_3-edge spectra (left) and second-derivative curves (right) for various Mo compounds. Raw data (—) and best fit (---). Top to bottom: Na_2MoO_4, $(NH_4)_2MoS_4$, $[N(Et)_4][MoOCl_4(H_2O)]$, $(PyH)_2MoOCl_5$, $LMoOCl_2$, $LMoSCl_2$.

The best fits are illustrated in Figure 5. Observed X-ray splittings are compared with those from optical spectra or calculations for the same Mo complexes and Tc analogues in Table I. Assignments have been made assuming that the ordering of X-ray transitions remains the same as for the optical spectra. The coordinate schemes used in the interpretation of these spectra are presented in Chart I.

L_3 and L_2 splittings of 2.48 and 2.19 eV were found for the tetrahedral $MoO_4{}^{2-}$ anion, substantially larger than one calculated $E - T_2$ splitting of 1.68 eV.[35] However, others have estimated $10Dq$ for $MoO_4{}^{2-}$ as 2.5–3.7 eV.[36] The mean $L_{2,3}$ splitting of 2.34 eV is very close to the reported values of ca. 2.33 eV for $TcO_4{}^-$, as expected in the effective field approximation. The average X-ray splitting of 1.37 eV for $MoS_4{}^{2-}$ is slightly higher than the ca. 1.23-eV optical value, but the comparable splitting for the $TcS_4{}^-$ anion is not known.

Quantitative interpretation of the oxychloride spectra is aided by reference to Chart II. The generally accepted ordering of d orbitals[37] has been assumed.
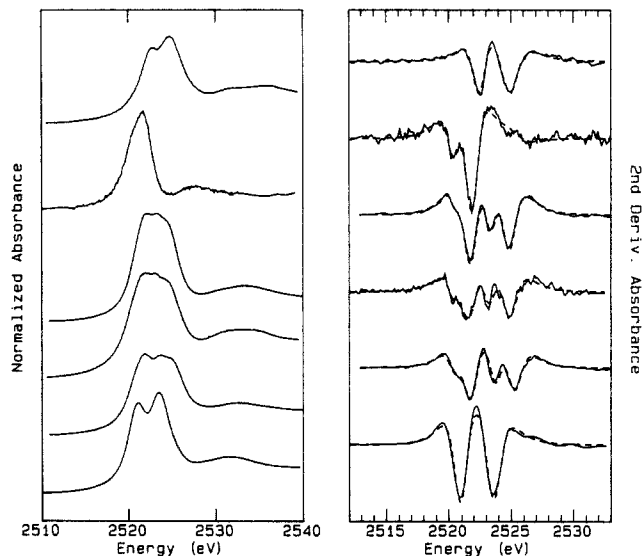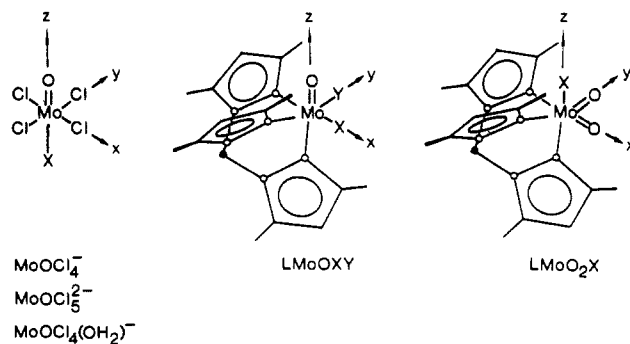
Chart I. Coordinate Schemes for Discussion of Mo Complex Spectra

$MoOCl_4{}^-$

$MoOCl_5{}^{2-}$

$MoOCl_4(OH_2)^-$

LMoOXY

$LMoO_2X$

An important difference between the X-ray and optical transitions involves the nature of the interelectronic repulsions in the excited state. In general, although the final-state d orbitals involved in transitions may be the same, the interelectronic Coulomb and exchange energies are different. A similar situation exists with ligand-to-metal charge-transfer (LMCT) spectra, in which the excited-state d count is higher than the ground state. In fact, the same theory of interelectron repulsions used for interpretation

(35) Kebabcioglu, R.; Müller, A. *Chem. Phys. Lett.* **1971**, *8*, 59.

(36) (a) Müller, A.; Diemann, E.; Jørgenson, C. K. *Struct. Bonding* (*Berlin*) **1973**, *14*, 23–47. (b) For a discussion, see: Lever, A. B. P. *Inorganic Electronic Spectroscopy*; Elsevier: Amsterdam, 1984; p 322.

(37) Winkler, J. R.; Gray, H. B. *Comments Inorg. Chem.* **1981**, *1*, 257–263.

Chart II. Schematic Illustration of Configurations and Interactions Important for Interpretation of Molybdenum Oxychloride Spectra (Separation of Orbitals Is Not to Scale)
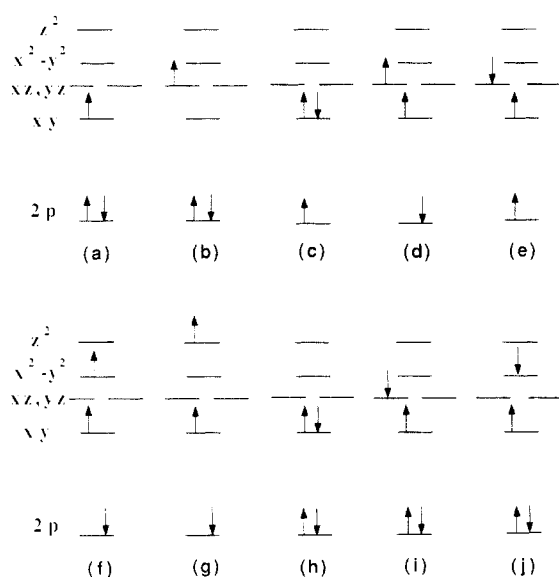
of optical spectra can explain the difference in line widths and the relationship between X-ray and optical transition energies.

In the following analysis it is assumed that the average X-ray splittings are given by

$$\Delta E_{\text{X-ray}} = \Delta E_{\text{orbital}} + \Delta J_{\text{d-d}} - \Delta K_{\text{d-d}} \tag{1}$$

where $\Delta E_{\text{orbital}}$, $\Delta J_{\text{d-d}}$, and $\Delta K_{\text{d-d}}$ are, respectively, the differences in orbital energies, Coulomb energies, and exchange energies between the excited and ground states. The use of an average X-ray splitting is admittedly empirical; a more detailed theory would have to account for the different splittings observed at the L_2 and L_3 edges.

The lowest energy optical d–d transition for the molybdenum oxychloride complexes corresponds to excitation from configuration 2a to 2b, whereas the first L-edge X-ray transition involves excited configuration 2c. For the X-ray transition there will be a repulsion between the promoted electron and the electron already occupying the d_{xy} orbital.[32,38]

For configuration 2b, exchange and Coulomb terms do not enter. Although d–d exchange interactions are absent in 2c, the Coulomb term is substantial, and for the filled d_{xy} orbital can be estimated by the Racah parameters $A + 4B + 3C$.[39] The Coulomb energy for the $d_{xy} - d_{xz,yz}$ interaction of Chart 2d is significantly smaller and can be approximated by Racah parameters $A - 2B + C$. In addition, an exchange term of $3B + C$ lowers the energy of 2d, but not 2e. Ignoring core–hole interactions and shell–shell terms, and assuming equal oscillator strengths for transitions to 2d and 2e, the X-ray splittings will be lower than the optical transitions by the difference in Coulomb energy ($6B + 2C$) plus half the exchange energy ($3B + C$)/2. Using the frequent assumption that $C = 4B$,[40] and a value for B of 436 cm^{-1} (0.054 eV),[41] yields an estimated difference between X-ray and optical splittings of 0.95 eV. The average first X-ray splitting of 0.99 eV in [MoOCl$_5$]$^{2-}$ is in fact lower by 0.72 eV from the optical value of 1.71 eV.

Sham has observed that the Ru L_3 edge $2p_{3/2} \rightarrow T_2$ feature is 1.0 eV sharper (fwhm) than the $2p_{3/2} \rightarrow E_g$ peak.[38] Similarly, the p $\rightarrow d_{xy}$ features in our oxychloride spectra are 1.0 eV sharper than transitions to the higher levels. In both cases, the broadening of the upper levels comes in part from exchange interactions that

are not present for transitions to a lower half-filled orbital.

For the $d_{xy} - d_{x^2-y^2}$ splitting, the d–d Coulomb energy for configuration 2f is estimated by $A + 4B + C$. The exchange energy in Racah parameters is given by $2C$. There can also be a transition to spin-paired analogues of configuration 2f, for which the exchange energy will not enter. An average energy difference for the X-ray vs optical transition splittings of $10B$ or 0.54 eV is calculated, slightly greater than the observed difference of 0.36 eV in [MoOCl$_5$]$^{2-}$. Similar calculations for the d_{z^2} transitions predict the average X-ray splitting to be reduced from the optical value by $20B$ or 1.08 eV. Unfortunately, there is no optical data for comparison.

Table I includes predictions for all of the optical transitions that can be calculated from the X-ray spectra. The average prediction proved to be low by 0.20 eV. Some of the discrepancy may result from our neglect of core–hole outer-shell interactions.

The d^2 Tc(V) transition from 2h to 2i involves approximately the same change in outer-shell orbital energy and Coulomb interaction as the difference in Mo X-ray transitions 2a–2e vs 2a–2c. However, the related X-ray transition 2a–2d has an exchange term, estimated by Racah parameters $3B + 2C$. Assuming this term lowers the average X-ray splitting by half the exchange energy, and using the same assumed parameters for Tc as for Mo, yields a predicted Tc optical transition of 0.99 eV (average Mo splitting) plus 0.19 eV (half-exchange energy), or 1.18 eV. This is in reasonable agreement with the observed Tc transition energy of 1.32 eV. The same arguments can be used to predict that the second X-ray splitting will have an energy equal to the average of the spin-allowed and spin-forbidden $d_{xy} \rightarrow d_{x^2-y^2}$ transition energies. The $L_{2,3}$ X-ray average splitting is 2.42 eV, compared to the optical average of 2.31 eV. Given the approximation involved, and the fact that technetium analogue bond lengths are not quite the same as the Mo structures, the agreement observed between experiment and prediction is quite encouraging.

The $L_{2,3}$ edges of LMoSCl$_2$ (Figure 5) illustrate the limitations of the technique. A fit to the derivative data resolves only two broad features, rather than four independent bands as in LMoOCl$_2$. Independent optical studies of this pair of complexes have shown that the ligand field splittings for LMoSCl$_2$ are much smaller than those for LMoOCl$_2$,[18] consistent with the L-edge results. However, in the absence of additional information (such as expected line widths) the L-edge spectra for LMoSCl$_2$ could be easily be misinterpreted as indicative of a higher symmetry species.

Orientation Dependence. The proposed assignments of Table I can be checked through the orientation dependence of single-crystal spectra.[42-44] In Figure 6a,b the spectra for a crystal of

(38) Sham, T. K. *J. Chem. Phys.* **1985**, *83*, 3222–3224.
(39) Lever, A. B. P. *Inorganic Electronic Spectroscopy*; Elsevier: Amsterdam, 1984; p 105. Racah parameters for molecules are empirical measures of electron–electron interaction energies.
(40) Lever, A. B. P. *Inorganic Electronic Spectroscopy*; Elsevier: Amsterdam, 1984; p 467.
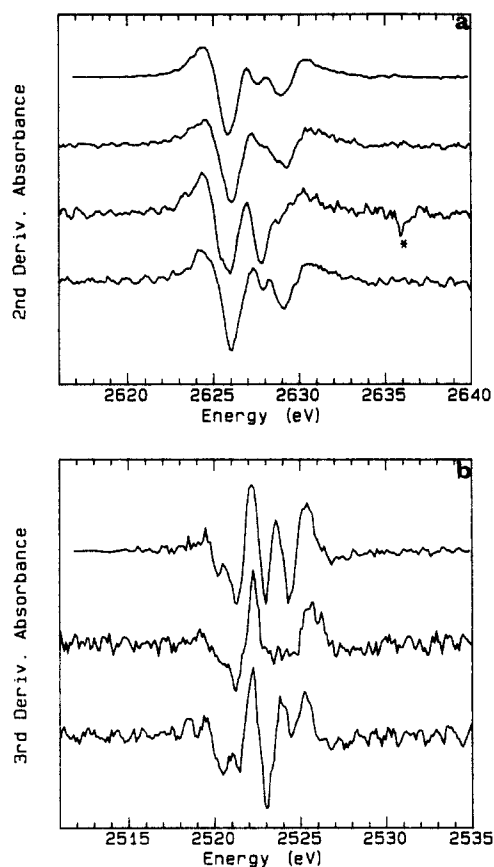(41) Mitchell, P. C. H. *J. Inorg. Nucl. Chem.* **1963**, *25*, 963.

(42) It is well-known that $L_{2,3}$ EXAFS has an orientation dependence given by

$$A(\theta) \propto 1 + 3 \cos^2 \theta$$

where θ is the angle between the absorber–scatterer axis and the polarization vector and $A(\theta)$ is the relative amplitude.[43] It is not well appreciated, however, that L-edge bound-state transitions can have a different orientation dependence. For example, although the angular dependence of the transition probability between the p orbitals and the d_{z^2} orbital is also given by

$$A_{d_{z^2}}(\theta) = 1 + 3 \cos^2 \theta$$

the angular dependence for transitions to the $d_{x^2-y^2}$ orbital is given by

$$A_{d_{x^2-y^2}}(\theta) = \sin^2 \theta$$

and the angular dependence for transitions to the d_{xz}, d_{yz}, and d_{xy} orbitals is given by

$$A_{d_{xz}}(\theta,\phi) = \sin^2 \theta \cos^2 \phi + \cos^2 \theta$$

$$A_{d_{yz}}(\theta,\phi) = \sin^2 \theta \sin^2 \phi + \cos^2 \theta$$

$$A_{d_{xy}}(\theta,\phi) = \sin^2 \theta$$

where θ and ϕ are the standard spherical polar coordinates defining the orientation of the polarization vector.[44] Since these expressions are averaged over all p-orbital initial states, additional angular dependence may arise from any selectivity conferred by fluorescence detection. They also do not include possible spin effects.

Figure 6. [N(Et)$_4$][MoOCl$_4$(H$_2$O)] crystal spectra. (a) L$_2$-edge (top to bottom) powder; $\vec{E} \parallel a$, $\vec{E} \parallel b$, $\vec{E} \parallel c$. (b) L$_3$ edge (top to bottom) powder; $\vec{E} \parallel a$; $\vec{E} \parallel b$. (c) Orientation of ions in unit cell. Oxygen atoms are highlighted. Ethyl groups on the cation are not shown; nitrogen atoms are included to show cation positions.

[N(Et)$_4$][MoOCl$_4$(H$_2$O)] are shown. As seen in the packing diagram of Figure 6c, the four Mo=O axes in the unit cell are nearly parallel to the *ac* plane and hence perpendicular to *b*. The relative intensity of the four components shows dramatic orientation effects, despite the fact that the Mo=O axes are not completely aligned.

For the highest energy transition, the minimum intensity occurs when the $\vec{E}$ vector is parallel to the *b* axis. If the d$_{z^2}$ orbital lies along the short Mo=O bond axis, then this is consistent with the tentative assignment, since all the Mo=O bonds in this crystal lie nearly parallel to the *ac* plane.

The next highest transition, assigned as p → d$_{x^2-y^2}$, has maximum intensity with $\vec{E}$ along the *b* axis. This is consistent with an orbital perpendicular to the Mo=O bond, but more quantitative analysis with a greater number of orientations is called for.

(43) Heald, S. M.; Stern, E. A. *Phys. Rev. B* 1977, 5549–5559.
(44) The calculations of *L*-edge angular dependence were kindly provided by Dr. Grant Bunker of the Institute for the Study of Function and Structure, Philadelphia, PA.
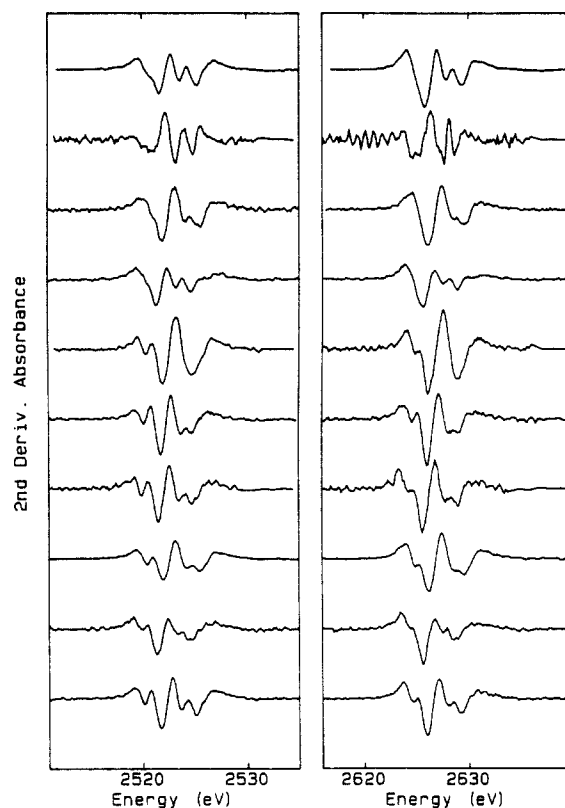

Figure 7. Ligand effects on Mo(V) complex L$_3$ edge (left) and L$_2$ (right) second derivatives. Samples were LMoOXY, where X, Y = (top to bottom): Cl, Cl; Cl, $^-$OCH$_3$; ($^-$OC$_6$H$_5$)$_2$; ($^-$SC$_6$H$_5$)$_2$; ($^-$OCH(CH$_3$)CH-(CH$_3$)O$^-$); ($^-$SCH$_2$CH$_2$S$^-$); ($^-$OCH$_2$CH$_2$S$^-$); ($^-$OC$_6$H$_4$O$^-$); ($^-$SC$_6$H$_3$-(CH$_3$)-o-S$^-$); ($^-$OC$_6$H$_4$S$^-$).

Significantly smaller polarization effects are observed for the next lowest band, which is again consistent with assignment as transitions p → d$_{xz,yz}$.

Finally, the lowest d orbital for the [MoOCl$_4$(H$_2$O)]$^-$ anion is the half-filled d$_{xy}$ orbital. Although a transition to this orbital is not resolved in the L$_2$-edge second derivative, a distinct feature can be observed in the L$_3$-edge third derivative in Figure 6b. As expected, this feature is polarized like the p → d$_{x^2-y^2}$ transition, along the *b* axis. The fwhm line width of this feature is 1.8 ± 0.3 eV, compared to values of greater than 3 eV for the other transitions.

Ligand Effects on L-Edge Splitting Patterns. The spectra of a series of oxomolybdenum(V) complexes, LMoOXY, where L = HB(Me$_2$pz)$_3$$^-$, and X, Y are various ligands are illustrated in Figure 7. A mutually cis configuration for the oxo group and the ligands X, Y is enforced by the sterically hindered ligand L. The effective site symmetry is C_s, and as many as four transitions are observed. Although the orbital pattern should resemble MoOCl$_5^{2-}$, the reduced symmetry allows significant d-orbital mixing, and we refer to these transitions in order of energy as p → ϕ_1, p → $\phi_{2,3}$, p → ϕ_4, p → ϕ_5. The dominant feature, p → $\phi_{2,3}$, corresponding to the deepest minimum in the second derivative, is assigned as transitions to a mix of nearly degenerate d$_{xz}$ and d$_{yz}$ orbitals. The next two features are assigned in order of increasing energy, to d$_{x^2-y^2}$ and d$_{z^2}$ orbitals. The ground state is expected to involve a half-filled predominantly d$_{xy}$ orbital, and in many cases a distinct low-energy feature can be observed.

Variation in the nature of X and Y changes the energies of all of the 2p → 4ϕ_i bands. Sulfur or chlorine ligands lower the average energy compared to oxygen for X and Y, but not all bands shift the same amount. For the complex with X = Y = Cl$^-$, the ϕ_5 - ϕ_4(d$_{z^2}$ - d$_{x^2-y^2}$) separation is 1.5 eV, and two well-resolved features are observed in the high-energy portion of the second-derivative curve. In contrast, the $^-$OCH(CH$_3$)CH$_2$(CH$_3$)O$^-$ ligand raises the ϕ_3 transition energy, more than the ϕ_4 level; thus the separation is only 1.0 eV and the transitions are resolved only by
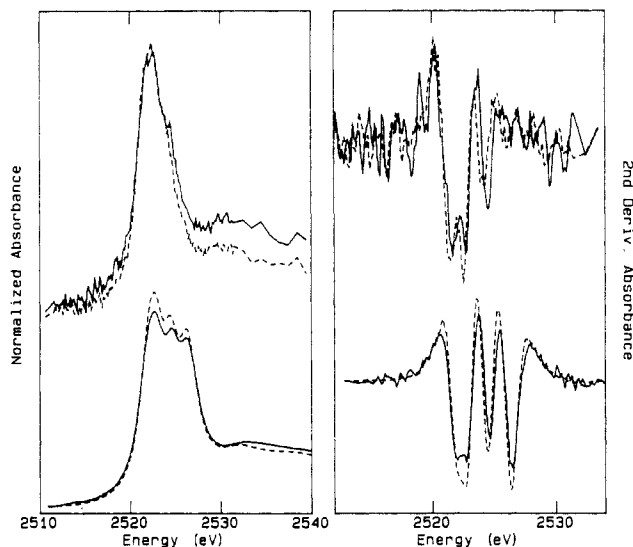
Figure 8. Oxo and halide effects on Mo(VI) L_3 edges (left) and second derivative curves (right). Top: $MoO(S_2CNEt_2)_2Cl$ (-) vs MoO-$(S_2CNEt_2)_2Br$ (---) Bottom: $LMoO_2Cl$ (-) vs $LMoO_2Br$ (---).

curve-fitting. The same pattern is observed between ($^-OC_6H_5$) ligands vs "softer" ($^-SC_6H_5$) ligands, or ($^-OC_6H_4O^-$) vs ($^-SC_6H_3(CH_3)$-o-S^-).

Constraining the geometry with bidentate ligands affects the $\phi_1 - \phi_{2,3}$ ($d_{xy} - d_{xz,yz}$) separation. For the complexes with X = Y = monodentate ligands, the splitting is not resolved in the second-derivative $L_{2,3}$-edge curves. Curve-fitting yields splittings of 1.26, 1.07, and 1.09 for the $(Cl)_2$, ($^-SC_6H_5)_2$, and ($^-OC_6H_5)_2$ complexes, respectively. When bidentate ligands are present, the $2p \rightarrow d_{xy}$ transition is invariably resolved from the $2p \rightarrow d_{xz,yz}$ transition, and splittings on the order of 1.5 eV are derived.[45]

Dioxomolybdenum(VI) complexes of the form $LMoO_2X$ (X = Cl$^-$, Br$^-$) have markedly different L-edge spectra from the monooxo Mo(V) complexes, as illustrated in Figure 8. For $LMoO_2Cl$, Fenske–Hall molecular calculations[46] using the co-ordinate system described in Chart I predict d-orbital energies in the order of $d_{xz} \approx d_{yz} < d_{xy} < d_{z^2} < d_{x^2-y^2}$. Thus, it is reasonable to assign the lowest energy feature as partially resolved $2p \rightarrow 4d_{xz,yz}$ and $2p \rightarrow 4d_{xy}$ transitions, the middle feature as $2p \rightarrow 4d_{z^2}$ and the highest feature as $2p \rightarrow 4d_{x^2-y^2}$. The latter feature is pushed to 2–3 eV higher than the d_{z^2} transition in the monooxo spectra. Presumably this reflects the strong repulsive forces felt by an orbital with two lobes directed at oxo groups.

The monooxo Mo(VI) halide complexes have distinctly different L-edge spectra. The highest energy transition is presumed to be approximately $2p \rightarrow 4d_{z^2}$, oriented along the Mo≡O axis, but the remaining features are poorly resolved.

Substitution of bromide for chloride has little effect on either type of oxo complex spectrum, as also shown in Figure 8. The corresponding band positions for the dioxo chloride and bromide complexes vary by less than 0.2 eV. Similarly, the monooxo Mo(VI) bromide spectrum strongly resembles the chloride spectrum.

The effects of replacing an oxo group with a sulfido ligand are illustrated in Figure 9. Two distinct changes are observed. First, the centroid of the transitions to the 4d level is shifted by ~ 1 eV to lower energy. Second, the splitting of the higher energy transitions, which is clearly visible in every oxo complex, is no longer resolved. It is reasonable to expect that a terminal oxo group causes a much larger splitting of the d_{z^2} and $d_{x^2-y^2}$ orbitals relative to a terminal sulfido group. This prediction is supported by results of Fenske–Hall calculations[46] and born out by the L-edge spectra. It is also worth noting that in the $LMo(O,S)(S_2CNEt_2)$

(45) Crystal structures are not yet available for any of the bidentate ligand complexes, and our assumptions about their structure are based on analogy with the complexes with monodentate ligands.

(46) Hall, M. B.; Fenske, R. F. *Inorg. Chem.* **1972**, *11*, 768.
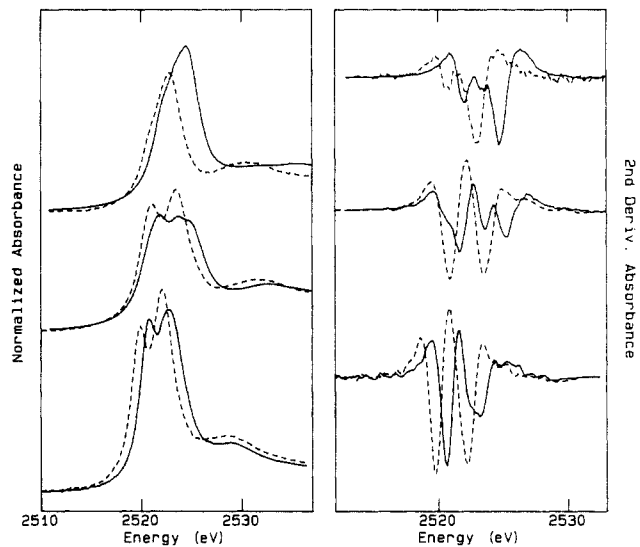

Figure 9. L-edge spectra (left) and second-derivative curves (right) for compounds with terminal oxo (—) vs terminal sulfido (---) ligands. Top to bottom: $MoO_2(pip)_2$ vs $MoS_2(pip)_2$; $LMoOCl_2$ vs $LMoSCl_2$; $LMoO$-(S_2CNEt_2) vs $LMoS(S_2CNEt_2)$.
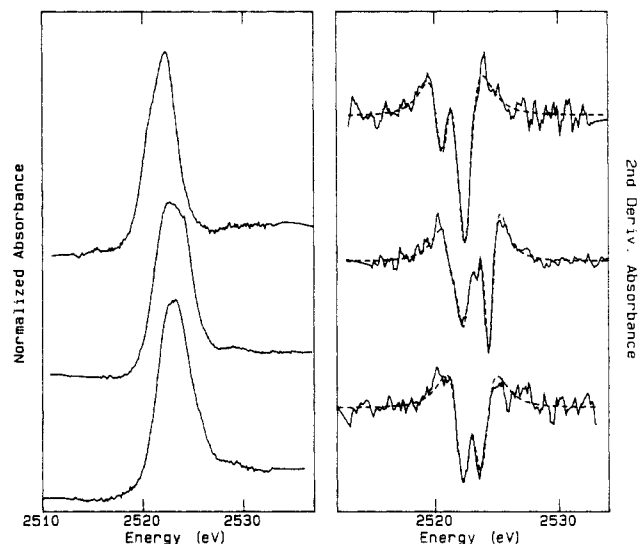

Figure 10. L_3-edge spectra (left) and second-derivative curves (right) for (top to bottom) dithionite-reduced nitrogenase, oxidized sulfite oxidase, and oxidized active xanthine oxidase.

spectra, the weak $2p \rightarrow 4d_{xy}$ transition is no longer observed, since the d_{xy} orbital is now filled. This further confirms the previous assignments.

Enzyme Spectra. The L_3 edges for dithionite-reduced nitrogenase, oxidized active xanthine oxidase, and oxidized sulfite oxidase are compared in Figure 10. For the first two enzymes, two major features are resolved by second-derivative curve-fitting, whereas for sulfite oxidase four distinct bands are observed. The first peak in the nitrogenase edges falls at 0.6 or 1.4 eV lower energy than the sulfite oxidase and xanthine oxidase spectra, respectively. The observed nitrogenase 1.7-eV splitting is slightly larger than the 1.4-eV active xanthine oxidase splitting, but both are much smaller than the 3.0-eV total splitting for sulfite oxidase.

The nitrogenase L_3 line widths are 2.7 and 3.1 eV for the lower and upper bands, respectively. At the moment, we cannot determine whether these widths represent broadening due to exchange interaction or a structural asymmetry that lifts orbital degeneracy. Since xanthine oxidase is d^0 Mo(VI) in the form examined, the observed lower and upper line widths of 2.7 and 3.2 eV in this case represent a structural broadening. The smaller overall splittings of xanthine oxidase vs sulfite oxidase are consistent with previous EXAFS results, which find oxo–sulfido

coordination for the former and dioxo coordination for the latter enzyme.[1]

Discussion

The Mo $L_{2,3}$ absorption spectra presented in previous sections appear to reflect the splittings of vacant d orbitals. Such an interpretation arises from a fortunate combination of circumstances. First, the interaction between the core p hole and the 4d electrons is small, compared to the ligand field splittings. Sham has estimated this interaction to be on the order of 0.1 eV in $Ru(NH_3)_6^{3+}$,[38] whereas in 3d transition metals the value is an order of magnitude greater.[47] Another important factor is that despite angular momentum selection rules, transitions to all orbitals are observed, at least for the Mo(V) and Mo(VI) oxidation states. This is in contrast to cases such as $Ru(NH_3)_6^{3+}$, where the L_2 and L_3 edges are dramatically different because of a forbidden $2p_{1/2}$ → t_{2u} transition at the L_2 edge. Finally, although the L-edge line widths are large compared to 3d K-edge spectra, second- and third-derivative spectra allow resolution of features that are barely discernable in the raw data.

The ligand field approach qualitatively explains the spectral features and their changes upon variation of X and Y for the $LMo^VO(XY)$ series of compounds. The strength of the Mo=O interaction raises the d_{z^2} orbital to a very high energy, ~ 4.5 eV above the half-filled d_{xy} orbital. The L-edge spectra show transitions to both of these orbitals, as well as intermediate bands corresponding to the $d_{xy,yz}$ pair and the $d_{x^2-y^2}$ orbital. Our spectral assignments are supported by the orientation dependence of [N-$(Et)_4][MoOCl_4(H_2O)]$ single-crystal spectra, which was generally in agreement with predictions.

A potential application of L-edge data is clarification of assignments made in optical spectroscopy. For example, a paper by Natkaniec and Jeżowska-Trzebiatowska[48] assigned a band at

20 600 cm^{-1} (2.55 eV) in the $TcOCl_5^{2-}$ spectrum to a d_{xy} → d_{z^2} ($2b_2$ → $8a_1$) transition. However, the L-edge 3.9–4.5-eV splittings for $MoOCl_5^-$ yield an estimated value of ~ 4.4 eV for the highest d_{xy} → d_{z^2} transition energy. Despite the uncertainty about converting X-ray levels into comparable optical values, it is clear that the 2.55-eV assignment is at far too low an energy, and that the band observed by Jeżowska-Trzebiatowska is more likely a d_{xy} → $d_{x^2-y^2}$ transition.

Conclusions

L-edge spectroscopy is clearly a useful probe for characterizing metal centers. In many cases, the correct number of bands predicted by a ligand field approach are observed, and when a smaller number of bands is seen, the effect can be attributed to splittings smaller than the experimental resolution. For quantitative agreement between X-ray and optical splittings, correction for Coulomb and exchange energies is required, just as for LMCT spectra. The smaller line widths, compared to K edges, make chemical shifts and changes in line shape more readily observable. The sharper features also yield better sensitivity to mixed species or contaminants, which are generally difficult for EXAFS to analyze or detect. L edges should thus prove useful for redox titrations of metal sites difficult to observe by more conventional spectroscopy. The sensitivity to geometric effects is a powerful complement to radial information derived from EXAFS. Combining such radial information with geometry-dependent molecular-orbital calculations and L-edge splittings may eventually lead to more complete structural predictions. Finally, if the appropriate corrections can be made, L-edge data are useful in interpretation of lower energy optical spectra.

Preliminary L-edge spectra of several Mo enzymes have been recorded, and the experimental sensitivity is certainly adequate for solution studies. Application of L-edge spectroscopy to metalloproteins bearing 3d transition metals is an obvious extension of the present work.

(47) Gupta, R. P.; Sen, S. K. *Phys. Rev. B* **1975**, *12*, 15–19.
(48) Natkaniec, L.; Jeżowska-Trzebiatowska, B. *Bull. Pol. Acad. Sci., Ser. Sci. Chim.* **1971**, *19*, 129–140.
(49) Müller, A.; Diemann, E. *Chem. Phys. Lett.* **1971**, *9*, 369–374.
(50) Garner, C. D.; Hill, L. H.; Mabbs, F. E.; McFadden, D. L.; McPhail, A. T. *J. Chem. Soc., Dalton Trans.* **1977**, 1202–1207.
(51) Gray, H. B.; Hare, C. R. *Inorg. Chem.* **1962**, *1*, 363.
(52) Astheimer, L.; Hauck, J.; Schenk, H. J.; Schwochau, K. *J. Chem. Phys.* **1975**, *63*, 1988–1991.
(53) Cotton, F. A.; Davison, A.; Day, V. W.; Gage, L. D.; Trop, H. S. *Inorg. Chem.* **1979**, *18*, 3024–3029.
(54) Jeżowska-Trzebiatowska, B.; Wajda, S.; Baluka, M.; Natkaniec, L.; Wojciechowski, W. *Inorg. Chim. Acta* **1967**, *1*, 205.
(55) Thomas, R. W.; Estes, G. W.; Elder, R. C.; Deutsch, E. *J. Am. Chem. Soc.* **1979**, *101*, 7863–7868.